Available online at www.sciencedirect.com

ScienceDirect

journal homepage: www.elsevier.com/locate/he

# Performance and bacterial enrichment of bioelectrochemical systems during methane and acetate production

*Nikolaos Xafenias*[*], *Valeria Mapelli*

*Industrial Biotechnology Group, Department of Chemical and Biological Engineering, Chalmers University of Technology, Gothenburg SE-41296, Sweden*

ARTICLE INFO

*Article history:*
Available online 4 June 2014

*Keywords:*
Microbial electrolysis cells
Carbon dioxide reduction
Bioelectrosynthesis
Methane
Acetate

ABSTRACT

A number of studies suggested that anaerobic digestion processes can be enhanced by inserting electrodes in anaerobic digesters, however a thorough work with relation to the bacterial shifts, especially with regards to acetogenesis, is lacking. In our work we investigated the performance and the respective shifts in the bacterial composition of bioelectrochemical systems producing methane and acetate from synthetic wastewater. A membraneless microbial electrolysis cell (MEC) could produce net energy with methane as the main end-product, however a membrane system was promoting acetogenesis and failed to operate as an energy producer. Bacteria present in the effluent of the membraneless system could also produce acetate with cathodic efficiencies over 60% when the cathode potentials dropped below −1000 mV vs. SHE. Different bacterial species were enriched on the two electrodes of each MEC, despite the fact that the electrodes were hydraulically connected and within a close distance from each other. *Acetobacterium* spp. and *Acetoanaerobium* spp., which could be found on the cathode of the membrane system, can be considered responsible for acetate production and decreased energy efficiency.



## Introduction

Bioelectrochemical systems (BES) have received a lot of research attention, especially during the last 15 years, representing a green energy technology that is capable of converting the chemical energy available in organic molecules into electrical energy, fuels, and commodities. Applications are very wide and vary from water and wastewater remediation [1,2], to powering implantable medical devices [3], and even to robotics [4] and mobile phone applications [5].

One way of extracting the chemical energy from wastewater and converting it into useful products is in microbial electrolysis cells, where hydrogen, methane and commodity chemicals are also produced in the cathodes [6]. Usually, microbial electrolysis cells (MECs) operate in the presence of a membrane separator to avoid mixing of the hydrogen produced in the cathode with carbon dioxide produced in the anode [7]. However, when methane is the target product in the cathode, the membrane can be removed in order to decrease the overall costs of the MEC, the pH gradients between the

* *Corresponding author*. Tel.: +46 704585557.
E-mail addresses: nxaf@hotmail.com, xafenias@chalmers.se (N. Xafenias).
http://dx.doi.org/10.1016/j.ijhydene.2014.05.038

anode and the cathode, and also the ohmic resistances of the system [8].

Bacteria are acting as bio-"catalysts" in MECs, and in addition to methanogenic archaea, they play a major role in methane formation, and therefore in the energy efficiency of these systems. However, their role in these systems varies; on one hand, bacteria can catalyze hydrogen production and/or scavenge toxic oxygen from the system [9–11], while on the other hand they can negatively affect the system by synthesizing products other than the ones desired (e.g. acetate). Because of the lack of membrane, an issue that might occur when membraneless MECs are designed for chemical oxygen demand (COD) removal is that acetate produced by homoacetogenic bacteria growing on the cathode [12], instead of methane and hydrogen, can cause an operation malfunction. Hydrogen and electrons used by autotrophic acetate producing bacteria might potentially decrease the energy efficiency of the system, and COD in the effluent will increase. A number of studies exist, where membraneless microbial electrolysis cells for hydrogen and methane production were used [8,13–25]. However, either because acetogenesis did not occur for a number of reasons in these studies, or because a bacterial analysis is lacking, the acetogenesis issue in membraneless MECs has not been properly addressed before.

Knowing how the reactor performance relates to changes in the bacterial populations and to what extent acetogenesis can affect the performance of these systems is important to define which are the microbial consortia and the related metabolic properties that favor specific MEC performances. For the above reasons, the aim of this study was to relate energy production and COD removal in biogas producing MECs with specific changes in the bacterial population. Operating issues with regards to acetogenesis are discussed, and we also demonstrate the effect of the electrode potential on the diversity of the bacterial populations thriving on the electrode surface under different MEC conditions. Our results provide information that could help to optimize energy efficiency and COD removal in MECs designed for wastewater treatment.

## Materials and methods

### *Reactor set-up*

*Microbial electrolysis cells*

Each MEC (Fig. 1(a)) was made by screwing together four poly(methyl methacrylate) plates (Plastmästarn AB, Sweden)

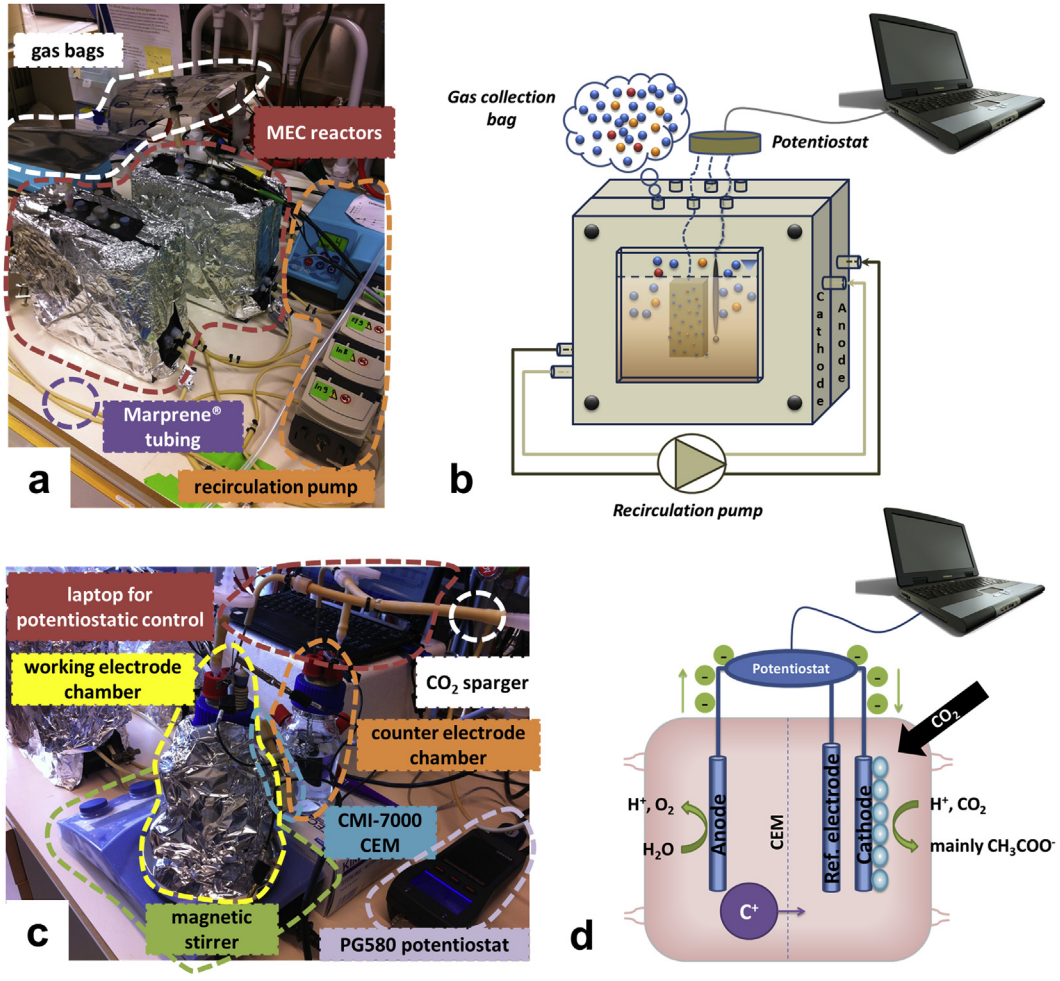


**Fig. 1 – Overview of the reactors used in this study; (a) the MEC reactors, (b) illustration of the MEC operation, (c) the potentiostatically poised H-type reactor, and (d) illustration of the H-type reactor operation.**

with dimensions 200 mm × 200 mm × 20 mm each. The two outer plates were completely compact, while each of the two inner plates had an inner gap with dimensions of 140 mm × 140 mm × 20 mm. This gave the reactors a total volume of 784 mL, and a working volume of 580 mL. Ethylene propylene diene monomer rubber gaskets (Ulinco AB, Sweden) were placed between the plates to prevent leakage. Five holes of 10 mm ⌀ and 30 mm length were drilled along the sides of each inner plate to pass the tubes used for recirculation, the gas collection bags, and the electrodes. The medium was continuously recirculated from the bottom to the top of the reactor, using a peristaltic pump (SciQ 323, Watson Marlow Ltd.) and Marprene® tubes with an inner diameter of 16 mm. Recirculation rate was approximately 0.35 working volumes per hour (200 mL $h^{-1}$). When used, a cation exchange membrane (CEM; CMI-7000, Membranes International Inc.) with a working surface area of 196 $cm^2$ was fixed between the two inner plates of the MEC reactor to separate the anode from the cathode. The membrane was kept immersed in a 0.5 M NaCl solution for several days to allow membrane expansion and hydration before use. Both working (WE) and counter (CE) electrodes were made of graphite felt (SIGRATHERM; SGL Carbon Ltd.) with dimensions of 100 mm × 80 mm × 5.5 mm and a total projected surface area of 180 $cm^2$. Graphite blocks were cut into rectangular cuboid pieces with dimensions of 100 mm × 6 mm × 3 mm each and were then fixed into the felt using an epoxy resin. A 0.8 mm titanium wire (2,67,902, Sigma–Aldrich) was used as the external circuit cable. The wire was covered with conductive silver epoxy (ITW, Chemtronics) and attached to the felt-block electrode by inserting it through a 1 mm hole drilled in the graphite block. The wire was then passed through a rubber bung that was closing one of the drilled holes and the bung was fixed to the reactor using epoxy resin. New electrodes were used in each reactor, after cleaning them sequentially with 1 N NaOH and 1 N HCl for 1 h each, and then storing them in milli-Q water which was replenished several times to allow neutralization of the water present in the felt's pores. Electrodes in MECs were placed within a 3 cm distance from each other. Carbon dioxide was sparged into the reactors before the start of each operation cycle and after emptying the gas collection bags.

H-type electrochemical reactors were assembled as shown in Fig. 1(b), in order to study cathodic current evolution individually. Two borosilicate bottles (Adams and Chittenden Scientific Glass, USA) with a working volume of 250 mL each were fixed together with a CEM (39 mm ⌀) that was placed in the middle. The same type of electrodes as in the MECs was used, and each electrode had a total projected surface area of 33 $cm^2$. Carbon dioxide was continuously sparged in the WE chambers of the H-type reactors to better control the pH (6.9 ± 0.1) and to continuously supply a carbon source to the microbial population.

Reference Ag/AgCl electrodes (3 M NaCl; RE-5B, BASi, UK) were passed through rubber bungs and inserted in the reactors from the top. These were used as reference electrodes (RE) versus which the WE potentials were controlled (+197 mV; all electrode potentials mentioned are vs. SHE). All experiments were conducted in a temperature regulated room (21 ± 1 °C) and the reactors were covered with aluminum foil to exclude light.

### Chemicals

A phosphate-buffered (pH 7) mineral medium was used in this work and this has been described elsewhere [8]. This medium was used both in the MECs and in the WE and CE chambers of the H-type reactors. Na-acetate (S2889, Sigma–Aldrich) was used as the electron donor and an additional carbon source in this study. Na-acetate was dissolved in the medium to make 200 g-$CH_3COO^-$ $L^{-1}$ solutions which were then stored at −20 °C until use. This solution was added in the MEC reactors to increase acetate concentrations to values between 1000–1500 mg $L^{-1}$ whenever acetate concentration dropped below 150 mg $L^{-1}$ pH adjustments in the membrane reactor between pH 7 and 8 were done manually using a 5 M HCl or a 5 M NaOH solution.

### Electrochemical monitoring and control

A three-electrode configuration was used along with a potentiostat in all instances, to monitor and control the WE potentials, and to record current produced under different applied conditions. A two-channel potentiostat (MLab; Bank Elektronik-Intelligent Controls GmbH, Germany) was used to control the MEC electrode potentials, while a single-channel potentiostat (PG580, Uniscan Instruments Ltd., UK) was used to control the half-cell electrode potentials. In chronoamperometry (CA) experiments current was recorded every 1 min and a multimeter was used to manually record the potential difference between the WE and the CE against the RE. Linear sweep voltammetry (LSV) and cyclic voltammetry (CV) experiments were performed at a scan rate of 1 mV $s^{-1}$, under quiescent conditions, and at least in duplicate. For the voltammetry experiments, the electrode potential remained at the starting potential for 1 min before start to minimize the non-Faradaic current shown in the graphs; current was recorded every 1 s in this instance.

### Analytical methods and calculations

Total suspended solids, total suspended volatile solids and total fixed solids were measured according to the Standard Methods 2540-D and 2540-E [26]. For the analysis of volatile fatty acids the samples were first centrifuged at 18,800 × *g* for 5 min. Volatile fatty acids were measured using a high-performance liquid chromatographer (Dionex Ultimate® 3000) equipped with a Rezex ROA-Organic Acids column (7.8 mm diameter, 300 mm length) kept at 80 °C; a 5 mM $H_2SO_4$ solution was used as the mobile phase with a flow rate of 0.8 mL $min^{-1}$. All target compounds were detected by a refractive index detector (RI-101; Dionex Corp., USA) and a variable wavelength detector (VWD 3100; Dionex Corp., USA) operating at the fixed wavelength of 210 nm.

Biogas was collected in gas bags and the volume was measured by the liquid displacement method. Methane, hydrogen, carbon dioxide, oxygen, and nitrogen gases were analyzed using a two-channel gas chromatographer (490 Micro GC, Agilent Technologies Sweden AB) which was equipped with a thermal conductivity detector. Channel 1 had a 10-m-long Molsieve 5 column, argon as the carrier gas (5.44 atm pressure), and was used for the analysis of methane,

oxygen, and nitrogen. Channel 2 had a 10-m-long CP-PoraPLOT U column, helium as the carrier gas (5.44 atm pressure), and was used for the analysis of hydrogen and carbon dioxide. A backflush time of 13 s, an injector temperature of 110 °C and a column temperature of 80 °C were applied to both channels.

Current density $j$ (A $m^{-2}$) was calculated as

$$j = \frac{I}{A_{el}} \quad (1)$$

where $I$ is the current recorded (A) and $A_{el}$ ($m^2$) is the electrode's total projected surface area.

Coulombic efficiency (%) was calculated assuming that acetate was the sole electron donor, as

$$CE = \frac{M\sum_0^{t_1} I\Delta t}{Fbv\Delta[CH_3COO^-]} \times 100\% \quad (2)$$

where M (59 g $mol^{-1}$) is the molecular weight of acetate ($CH_3COO^-$), $I$ (A) is the current recorded within time $\Delta t$ (sec), $F$ (96,485.3 Coulombs $mol^{-1}$ of electrons) is the Faraday's constant, b (8 moles of electrons) is the number of electrons exchanged per mol of $CH_3COO^-$, $v$ (L) is the working volume of the reactor, and $\Delta[CH_3COO^-]$ is the reduction of $CH_3COO^-$ concentration (g $L^{-1}$) within time $t_1$.

Net power produced over time $t_1$ (h) was calculated as

$$P_{net} = \frac{10.3\ (\text{Wh L}^{-1}) \times V_{CH_4}}{t_1} + \frac{3.3\ (\text{Wh L}^{-1}) \times V_{H_2}}{t_1} - V \times I \quad (3)$$

where 10.3 and 3.3 (Wh $L^{-1}$) are the combustion energies of methane and hydrogen respectively at $T = 21$ °C and $P = 1$ atm, $V_{CH4}$ and $V_{H2}$ (L) are the volumes of methane and hydrogen produced within the time interval $t$, $V$ (Volts) is the average potential difference between the working and the counter electrode for the time interval $t_1$, and $I$ (A) is the current recorded during the time interval $t_1$. In order to compare net power produced by the MECs with that of the control reactor without poised electrodes, $P_{net}$ (W $m^{-3}$) was normalized by the reactor working volume ($m^3$):

$$P_{net-V} = \frac{P_{net}}{v} \quad (4)$$

The methane yield was calculated over the time period $t_1$ as

$$Y_{CH_4} = \frac{V_{CH_4}}{\Delta COD_{acet}} \quad (5)$$

where $V_{CH4}$ (L) is the volume of methane produced during time period $t_1$ and $\Delta COD_{acet}$ (g) is the mass of the acetate consumed during time $t$, expressed as COD. The relationship between COD and acetate consumption (64 g COD = 60 g acetate) is given according to the following reaction:

$$CH_3COOH + 2O_2 = 2CO_2 + 2H_2O \quad (6)$$

### Inoculation and startup

Anaerobic sludge originating from the mesophilic (37 °C) sludge treatment process of Gothenburg's wastewater treatment plant (Gryaab AB) was used as inoculum to give an initial total volatile suspended solids concentration of 2498 ± 68 mg $L^{-1}$ in all MEC-type reactors. After inoculation, the anodes of the MECs were poised at +200 mV during a startup period, until stable current was produced for at least two acetate spiking cycles. From that time forward, the anode potential was reduced by 100 mV down to −100 mV, and each potential was applied for a period of 7–10 d. Inoculation of the WE chamber of the H-type cell was done twice (on days 0 and 2) with 50 mL of effluent from the membraneless MEC reactor, at the end of the MEC operation.

### Microbial community analysis

At the end of operation, electrodes were taken out of the reactors and three sample pieces of approximately 1 cm × 1 cm were cut from the top left, the middle, and the bottom right of each electrode. Microbial biomass from sludge and suspension samples was harvested via centrifugation and removal of the supernatant, while microbial biomass from the electrodes was harvested by 5 vortexing cycles of 1 min each, after addition of the sodium phosphate buffer provided with the DNA extraction kit. Genomic DNA extraction was performed using FastDNA™ SPIN Kit for Soil (MP Biomedicals, LCC), by following the instructions of the manufacturer. 16S rDNA was amplified from extracted DNA via PCR using the forward primer 5′-AGAGTTTGATCCTGGCTCAG-3′ [27] and the reverse primer 5′-CTACGGCTACCTTGTTACGA-3′, which is a modified version of the 1494R primer [28]. Both primers were phosphorylated at 5′ (Eurofins MWG Operon, Germany). Phusion High fidelity DNA polymerase (Thermo Fischer Scientific, Inc.) was used for amplification of the 16S rDNA. The 16S rDNA was purified (Illustra™ GFX™ PCR DNA and Gel Band Purification kit, GE Healthcare) and cloned at the SmaI restriction site into the plasmid pBluescript SK(+) [29]. Competent *Escherichia coli* DH-5α cells (Invitrogen™) were transformed and plated on LB-Agar plates containing 100 μg $mL^{-1}$ ampicilline, 40 μg $mL^{-1}$ X-GAL (5-bromo-4-chloro-3-indolyl-β-D-galactopyranoside) and 0.5 mM IPTG (Isopropyl β-D-1-thiogalactopyranoside). White colonies were picked and grown in 96-well sterile plates. Partial sequencing of cloned 16S rDNA was performed (GATC Biotech AG, Germany) and sequences were analyzed and classified using the Ribosomal Database Project (RDP) [30] with a bootstrap confidence of 80% [31].

## Results

### MEC performance

Our initial design was planned to compare methane and acetate production, COD reduction, and microbial enrichment between a membrane and a membraneless MEC. However, in a preliminary experiment with a CEM as the separator of a dual-chamber MEC operating in fed-batch mode with a biological cathode, the CEM failed to keep a pH balance in the system (data not shown). Despite manually adjusting the pH in the anode and cathode, the presence of the membrane led to a high divergence between the anodic pH (6.8 ± 0.8) and the cathodic pH (8.0 ± 1.1). Eventually, these pH imbalances caused a current inhibition and a system failure. In order to allow comparison with the membraneless MEC, the

membrane MEC experiment was repeated up to the time point where pH gradients started to build up. At that point, the membrane was sliced (35 $cm^2$ opening) to allow more sufficient transfer of protons [8,32], and to test whether the different conditions implied due to the membrane could lead to differences in the efficiency and/or the microbial diversity of this MEC reactor, compared to a membraneless MEC reactor.

As can be seen in Fig. 2(a), maximum current densities were observed at the anodic potential of +100 mV for both the membraneless and the sliced membrane MECs ($1.37 \pm 0.50$ A $m^{-2}$ for the membraneless and $1.84 \pm 0.38$ A $m^{-2}$ for the sliced membrane reactor). Current produced was higher for the sliced membrane reactor at the anode potentials of +200 and +100 mV, however at values comparable to those of the membraneless reactor. On the other hand, acetate removal was always lower for the sliced membrane reactor (167–298 g $m^{-3}$ $d^{-1}$ vs. 234–332 g $m^{-3}$ $d^{-1}$; Fig. 2(b)), and it was not directly following the higher current produced by this reactor at the anode potentials of +200 and +100 mV. In addition, a membraneless reactor operating without potentiostatic control removed acetate at considerably lower rates than both other reactors (85 g $m^{-3}$ $d^{-1}$). The potentials applied on the cathodes were lower in the sliced membrane reactor at all times (−919 mV ± 40 mV to −1075 mV ± 63 mV vs −863 mV ± 65 mV to −920 mV ± 21 mV; Fig. 2(c)), also because of the higher pH maintained in the cathode of this reactor; that was 8.1 ± 0.6, compared to the lower 7.5 ± 0.4 that was observed in the anode part, despite the tear in the membrane. On the other hand, the pH did not vary considerably in the membraneless reactor and remained at 7.7 ± 0.3 during the entire operation. In comparison, the pH in the membraneless reactor without potentiostatic control was relatively stable at 7.1 ± 0.3. In Fig. 2(d) the Coulombic efficiencies of the two reactors are shown. These were between 70 and 96% in the membraneless reactor, however in the sliced membrane reactor they were always higher than 100% (107–140%) because of electrons recirculated back to the anode in the form of acetate (Eq. (2)), as also discussed in the "Discussion" section.

Power produced as methane is presented in Fig. 3(a and b). As can be seen, methane production in the membraneless reactor (Fig. 3(a)) did not vary considerably for the three anode potentials reported, and ranged from 33 to 37 W $m^{-3}$. This can be compared to the 16–19 times lower power produced as methane in the control reactor without potentiostatic control (only 2 W $m^{-3}$), indicating very limited methanogenesis and power production in the absence of polarized electrodes. In the membraneless reactor, hydrogen production was considerably lower than methane production, with power produced from hydrogen ranging from only 1 W $m^{-3}$ to 2 W $m^{-3}$; in comparison, hydrogen production by the control reactor was almost zero. Power produced from methane in the sliced membrane reactor (Fig. 3(b)) was from 2 (anode potential of +100 mV) to 13 times (anode potential of −100 mV) lower than the power produced by the membraneless reactor; hydrogen production was also negligible in this instance. A comparison of the methane yields is made in Fig. 3(c). As can be seen, the membraneless reactor had a methane yield ranging from 0.25 to 0.31 L-$CH_4$ $g^{-1}$-COD removed as acetate. This was considerably higher than the 0.03–0.13 L-$CH_4$ $g^{-1}$-COD removed as acetate observed in the sliced membrane reactor and the

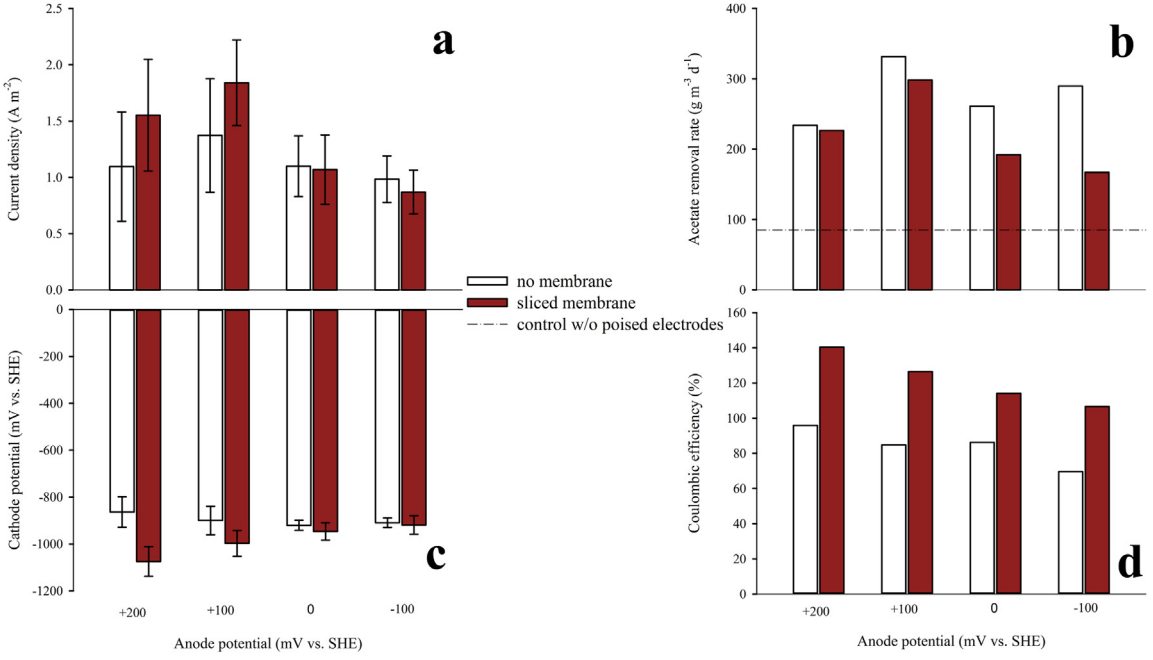


**Fig. 2 – Performance parameters of the two MEC reactors running for 7–10 d at each anode potential; (a) current densities produced, (b) acetate removal rates- comparison with the control reactor without potentiostatic control (dashed line), (c) cathodic potentials applied, (d) Coulombic efficiencies. Error bars in (a) represent the standard deviations from the current measurements recorded every 1 min and in (c) they represent the standard deviations of the cathode potential measurements taken manually ($n = 11–20$).**

0.12 L-$CH_4$ $g^{-1}$-COD removed as acetate observed in the control reactor without poised electrodes. Net power produced or consumed by the three reactors is shown in Fig. 3(d). As can be seen, net power (7–10 W $m^{-3}$) was produced by the membraneless reactor at anode potentials equal or lower than 0 mV, and this was 4–5 times higher than the net power produced by the control reactor without potentiostatic control (only 2 W $m^{-3}$). On the contrary, the sliced membrane reactor could not produce net power under neither potential, mainly because of the low methane volumes and yields observed. Approximately 19–43 mW $m^{-3}$ were being consumed by this reactor, which finally failed to operate as an energy producer. This was most probably because acetate was being produced on the cathode with an expenditure of power, as indicated by the low acetate consumption rates, the low methane and hydrogen production rates, but also by the microbiological analysis presented and discussed in paragraphs 3.3 and 4.

The CVs of the potentiostatically controlled electrodes are compared with the CVs of the reactor without potentiostatic control at the end of the operation period, in Fig. 4. As can be seen, while the microbial population in the control reactor could not produce catalytic current by that time, all biofilms on the potentiostatically controlled electrodes demonstrated a noteworthy electrocatalytic behavior. Furthermore, there was a significant difference in the behavior between the anodic (Fig. 4 (a and c)) and cathodic biofilms (Fig. 4 (b and c). While catalytic current could be produced from the anodes at electrode potentials over −300 mV, that was not possible for the cathodes which on the other hand produced a major catalytic wave at potentials lower than approximately −800 mV. This showed that the microbes on the anode and cathode electrodes could be assigned two distinct roles: donating or accepting electrons, to and from the electrodes, respectively.

### *H-type reactor performance*

As discussed earlier, the membraneless system demonstrated an enhanced methane production and could operate as an energy producer. To investigate whether acetogenesis could potentially occur under favorable conditions, we studied the cathode conditions individually. For this reason, we inoculated the working electrode of an H-type cell with effluent from the membraneless reactor. To make sure that the low current produced during the first two days of operation was not due to insufficient amount of biomass, a second inoculation followed on day 2 of the operation.

The performance of the half-cell cathode is shown in Fig. 5. As can be seen in Fig. 5(a), when the WE was poised at −900 mV, current production increased, however at rates that were considerably slower than when the lower potentials of −1000 mV and −1100 mV were applied. No considerable amounts of formate or propionate were produced at any

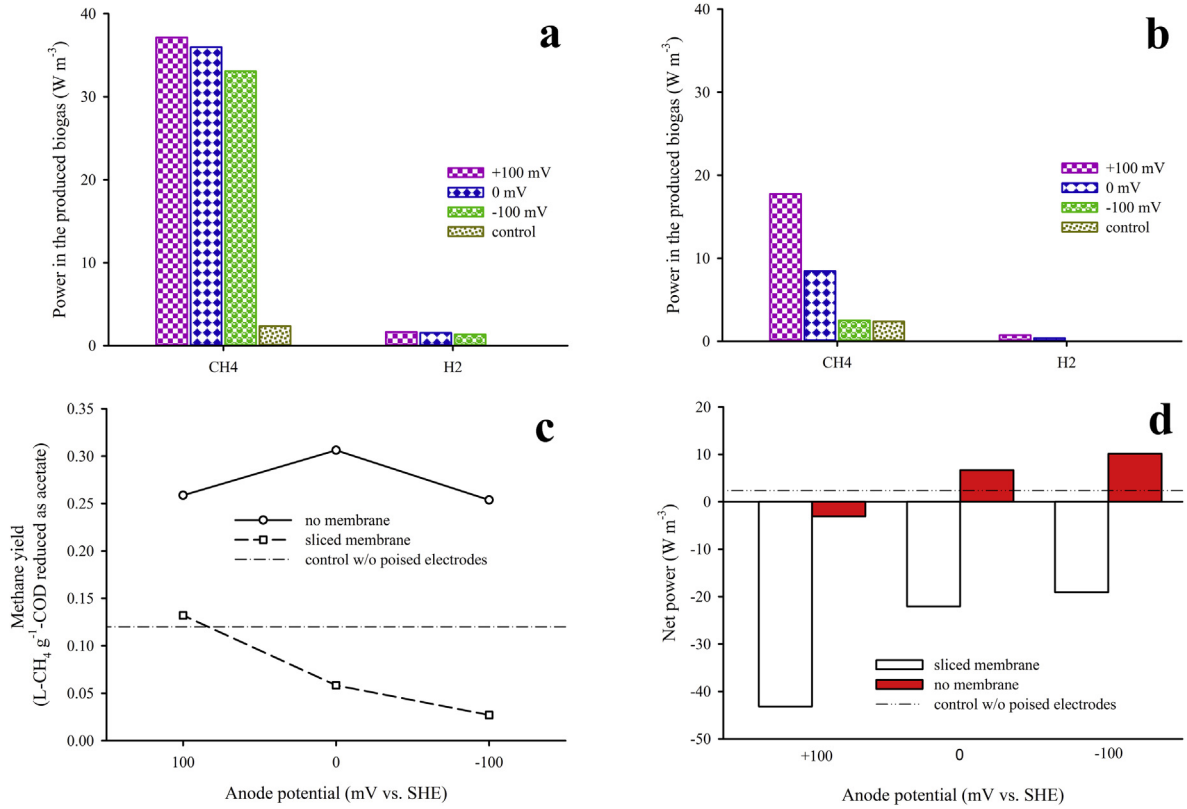


**Fig. 3 – Power considerations for the two MEC reactors and their control reactor without potentiostatic control; (a) power produced by methane and hydrogen in the membraneless MEC reactor and in the control reactor, (b) power produced by methane and hydrogen in the sliced-membrane MEC reactor and in the control reactor, (c) methane yield with respect to the anode potential in both MECs- comparison with the control reactor (dashed line), (d) net power produced or consumed by both MECs with respect to the anode potential- comparison with the control reactor (dashed line).**

electrode potential (Fig. 5(b)), however net production of acetate started at working electrode potentials equal or lower than −1000 mV. This was at the rates of 52.6 mmoles acetate $m^{-2}$ $d^{-1}$ at −1000 mV and at the rates of 171.4 mmoles acetate $m^{-2}$ $d^{-1}$ at −1100 mV. In other terms, at least 60% of the electrons traveling from the CE to the WE were used for acetate synthesis at −1000 mV; this percentage increased to 65% at −1100 mV, indicating that acetogenesis was not only possible, but was also more efficient with decreasing potentials.

Fig. 5(c) shows the voltammograms produced at different times of the operation. As can be seen, catalytic current was only slightly produced after 19 d of operation at −900 mV, and had an onset at approximately −800 mV. As the electrode was operated at the lower potentials of −1000 mV and −1100 mV, a second onset could be observed approximately at −300 mV. Though the latter onset produced a relatively limited current, it could be related to the reduction of $CO_2$ to methane ($E' = -237$ to −303 mV for pH 7–8) or acetate ($E' = -287$ to −352 mV for pH 7–8), but not to the reduction of $H^+$ to hydrogen ($E' = -409$ to −467 mV for pH 7–8) (redox potentials calculated from the Nernst equation for $T = 21\ ^\circ C = 294.15$ K). Also, as can be seen in Fig. 5(d), some electrocatalytic activity could be observed on the cell-free supernatant (after cell removal via a 0.2 μm filter) by using a clean electrode. Again an onset of catalytic current was observed at approximately −300 mV and this is an indication that compounds excreted by the microbial population could electrochemically interact with the poised electrode at potentials equal or lower than −300 mV.

### *Microbial enrichment*

Proteobacteria was the dominating bacterial phylum in the mesophilic anaerobic sludge used for the inoculation of all MEC-type reactors, representing 51% of the total analyzed population (Fig. 6(a)). The enrichment and selection process that occurred in the different MEC reactors is substantial and becomes more clear by comparing the patterns of the bacterial classes (Fig. 6(b)). While only one out of 278 16S rDNA sequences analyzed could be assigned to the δ-Proteobacteria class (*Syntrophorhabdus* genus), α-, β- and γ-Proteobacteria were similarly distributed (Fig. 6(b)). Nonetheless, δ-Proteobacteria represented 92 and 95% of the Proteobacteria on the anodes of the membraneless and the sliced membrane reactor, respectively (Fig. 6(c)), showing how the specific anodic environments contributed to the enrichment of specific populations. In particular, the classified δ-Proteobacteria mainly belonged to the *Geobacter* genus (83–85% of the total δ-Proteobacteria). γ-Proteobacteria were dominant on the cathode of the sliced membrane MEC and they were mainly represented by the *Pseudomonadaceae* family (59% of the total cathodic bacterial population). Bacteroidetes phylum was also enriched in all the reactors, when compared to the original sludge. A specific selection occurred within the Firmicutes phylum: Bacilli and Clostridia classes were present in the starting sludge (Fig. 6(b)), however only Clostridia could be identified in all the reactors among the classified Firmicutes. Furthermore, in the starting sludge, on both electrodes of the membraneless MEC, and on the anode of the two-chamber MEC, classified Clostridia belonged to the families of

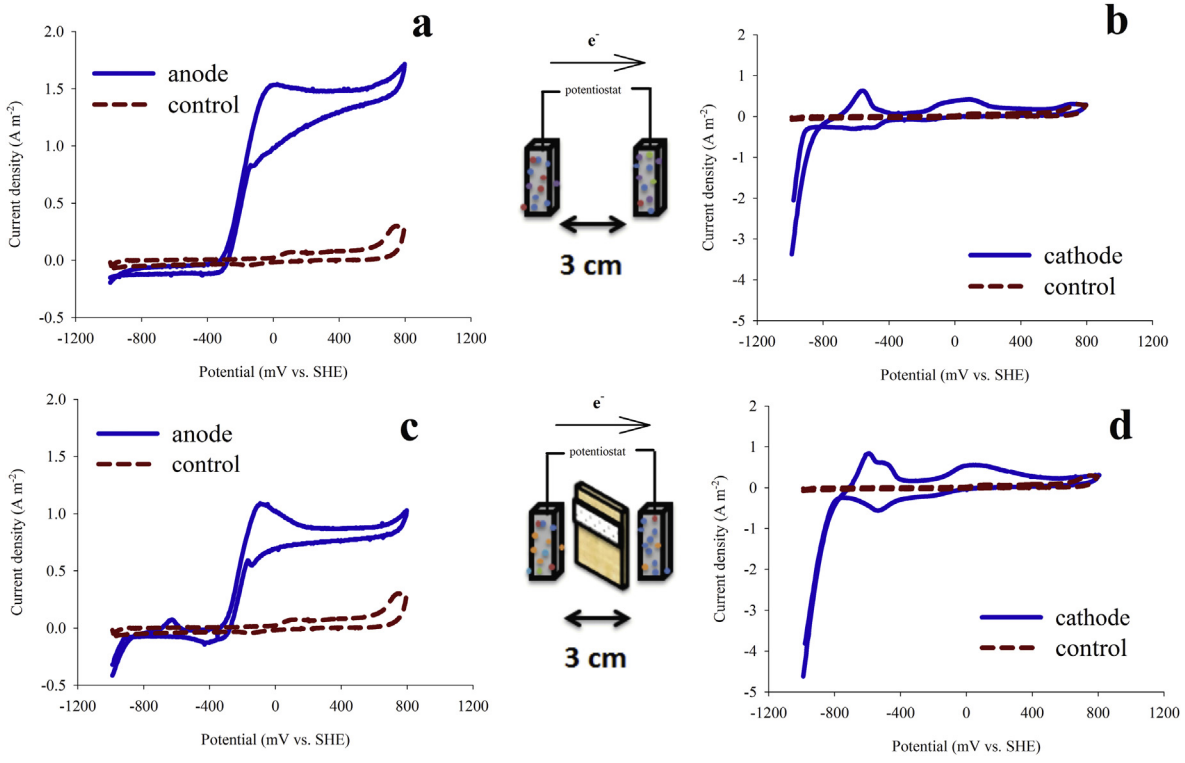


**Fig. 4 – Cyclic voltammograms recorded under turnover conditions at the end of the operation period from the two MECs and the control reactor without any potentiostatic control; a) anode and b) cathode of the membraneless reactor, c) anode and d) cathode of the sliced-membrane system.**

*Clostridiaceae*, *Peptostraptococcaceae*, *Clostridiales incertae saedis*, and *Ruminococcaceae* (Fig. 6(d)); on the other hand, only Clostridia that belonged to the *Acetobacterium* spp. and *Acetoanaerobium* spp. genera (i.e. *Eubacteriaceae* family) were found on the cathode of the dual-chamber MEC. Interestingly, although the inoculum of the H-type reactor derived from the effluent of the membraneless MEC, where the analysis of the 16S rDNA sequences could not lead to the identification of members of the *Eubacteriaceae* family, *Acetobacterium* spp. represented 56% of the total bacterial population and 100% of the total Firmicutes thriving on the working electrode of the H-type reactor.

## Discussion

In this work we evaluated the energy generated from synthetic wastewater in MECs, with respect to the reciprocal relationship between the MEC performance and the microbial consortia colonizing the electrodes. In connection with the microbial diversity, the performance of the MEC reactors differed to a considerable extent, despite the similarities in the operating conditions (i.e. inoculum, anodic potentials, medium, temperature, etc.). An increased methane production and acetate reduction was shown in both MEC setups, compared to the reactor without potentiostatic control. However, a positive energy outcome could be obtained only from the membraneless MEC, mainly because in this instance the cathode potentials applied resulted in limited or no acetogenesis, and therefore the electrons ended up in the gaseous energy carriers hydrogen and methane instead of acetate. This finding is important because it clearly shows that net power can be produced and COD reduction can be enhanced in MECs, without the need of expensive membranes or a complex design.

In the sliced membrane reactor, the more alkaline pH in the cathode (due to insufficient transfer of protons from the anode), the probably increased internal resistances imposed by the membrane, and the higher current demands from the anode, caused low cathode potentials. These conditions seemed to encourage the growth of acetate producing *Acetobacterium* spp. on the cathode surface, which were recirculating electrons from the cathode to the anode in the form of acetate. This caused higher (over 100% at all times) Coulombic efficiencies and also lower net acetate consumption rates in this reactor, compared to the membraneless MEC, despite the similar current values produced. Coulombic efficiencies were higher with lower cathode potentials, showing that electrons were recirculated from the cathode back to the anode via electron carriers, whose production was more efficient with

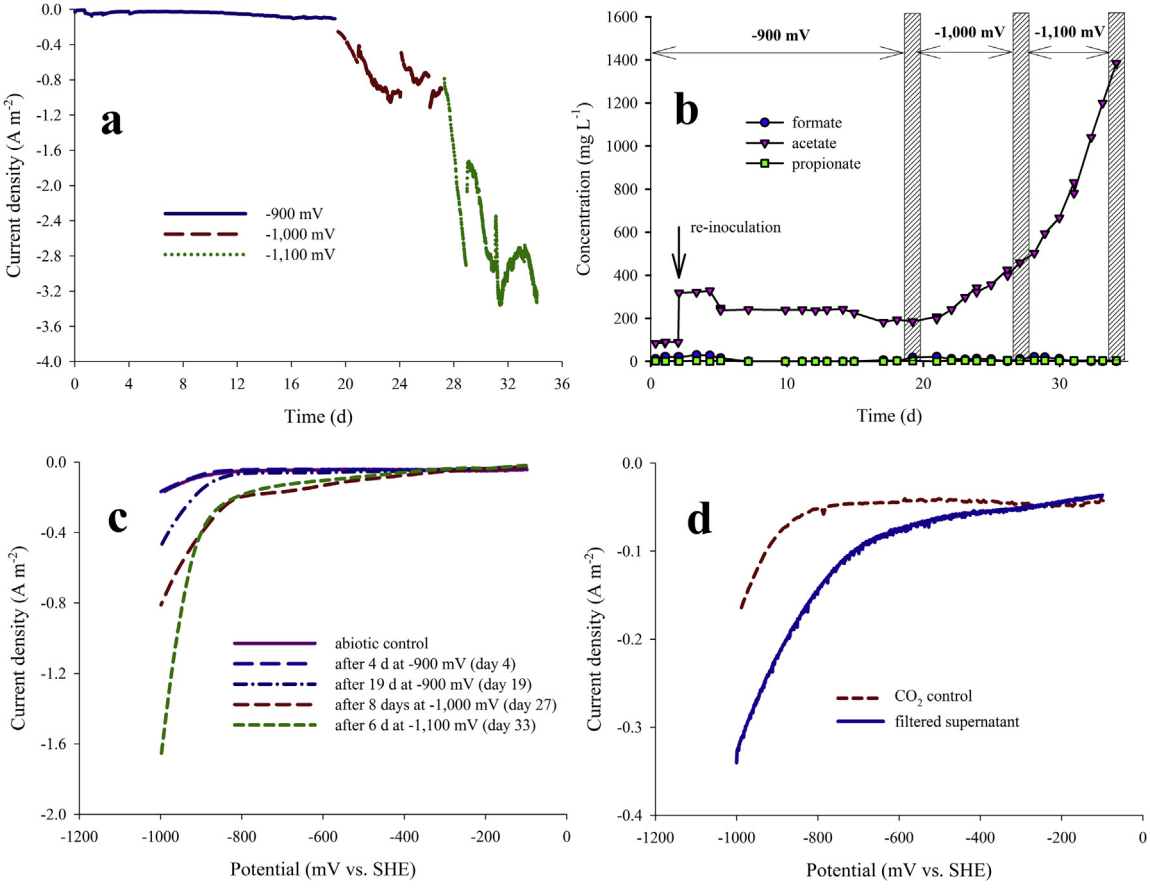


**Fig. 5 – Performance of the half-cell cathode; (a) current production under three different applied potentials, (b) formate, acetate, and propionate concentrations, (c) LSVs showing the evolution of the cathodic catalytic activity with time, (d) LSV of the abiotic filtered supernatant and comparison with that of an abiotic control with only the nutrient medium. $CO_2$ saturated conditions were maintained during all the voltammograms presented in this figure.**

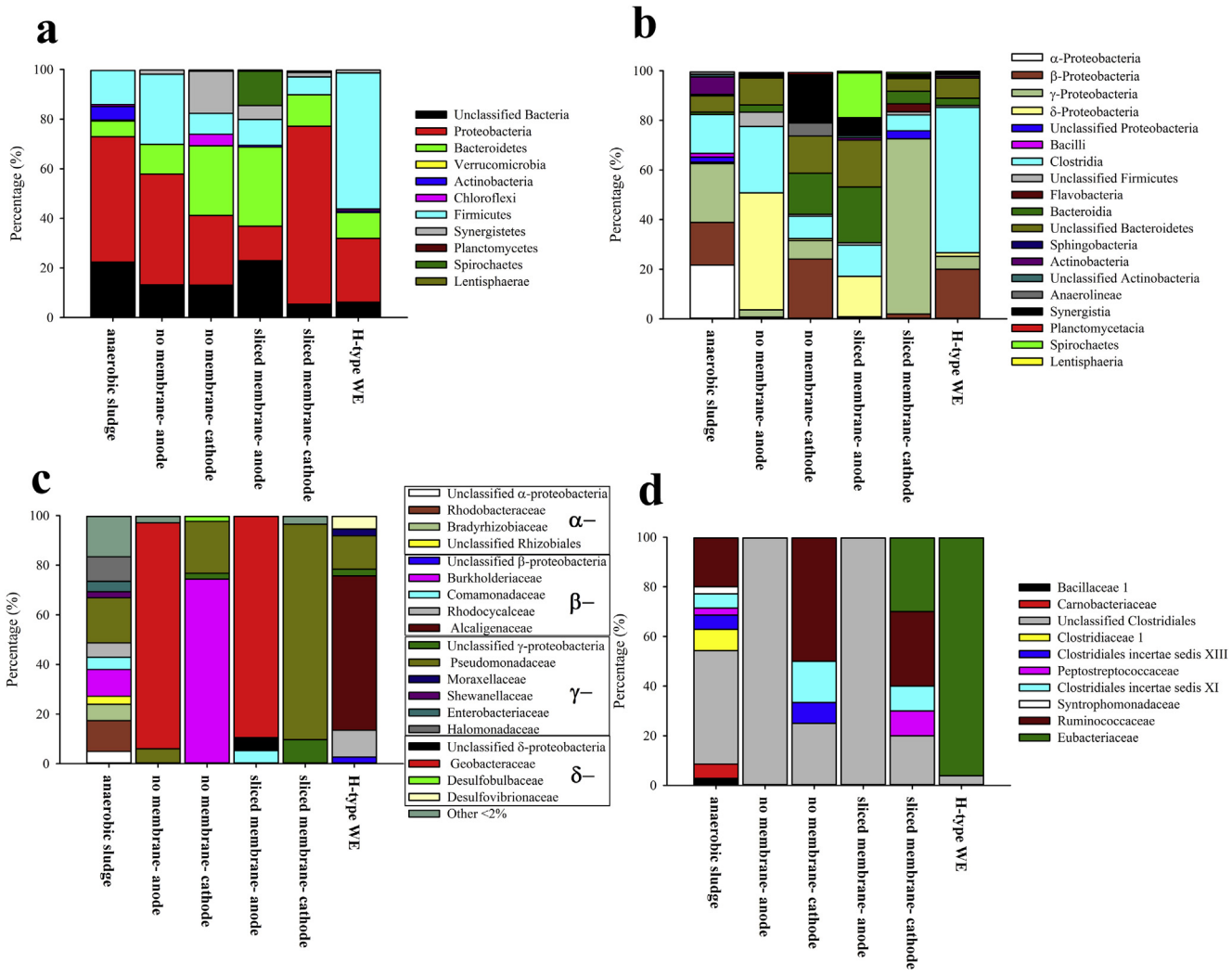


**Fig. 6 – Microbial analysis of the anaerobic sludge, the anode and cathode electrodes in the membraneless reactor, the anode and cathode electrodes in the sliced membrane reactor, and the H-type WE; a) phylum distributions, b) class distributions, c) Proteobacteria families distributions (families represented with less than 2% include *Acetobacteraceae*, *Methylobacteriaceae*, *Phyllobacteriaceae*, *Methylocystaceae*, *Rhizobiales incertae sedis*, *Sphingomonadaceae*, unclassified *Sphingomonadales*, unclassified β-Proteobacteria, *Neisseriaceae*, unclassified γ-Proteobacteria, *Moraxellaceae*, *Aeromonadaceae*, *Xanthomonadaceae*, *Syntrophorhabdaceae* in the anaerobic sludge; *Alcaligenaceae*, *Desulfuromonadaceae* in the membraneless anode; *Comamonadaceae*, *Xanthomonadaceae* in the sliced membrane cathode), and d) Firmicutes families distributions.**

lower cathode potentials. High Coulombic efficiencies could be explained only by hydrogen recirculation back to the anode [21], however our microbiological analysis together with the reported reactor performance (e.g. acetate reduction rates, Coulombic efficiencies) clearly showed that acetogenesis, under favorable conditions, is also a reason for electrons recirculation back to the anode. In addition, methanogenesis was not the dominant cathodic pathway in the sliced membrane MEC, and methane yield was only up to 34% of the theoretical maximum value (0.38 L-$CH_4$ $g^{-1}$-COD at 21 °C) and close to the yield observed in the control reactor (32% of the maximum value).

The membraneless reactor managed to operate as an energy producer and methanogenesis was the dominant cathodic pathway. In this instance, the calculated Coulombic efficiencies were in the range of the values expected in MECs where methanogenesis is dominant [8]. In addition, the methane yield was relatively high and up to approximately 82% of the theoretical maximum value, proving that methanogenesis was more efficient in the membraneless reactor than in the sliced membrane MEC and in the control reactor.

The enrichment process of the microbial populations in the MECs was very much affected by the electrode conditions applied. As a result, the diversity of the microbial communities thriving on the electrodes was significantly different from the diversity of the starting inoculum, and also remarkable differences in the community composition could be observed when comparing anodes and cathodes. This is

remarkable, especially considering that the electrodes were very close to each other and that the MECs were inoculated with the same starting inoculum that was continuously mixed. While it is possible that microbial communities developed on the anodes and cathodes of single-chamber microbial fuel cells do not differ significantly [33], the considerably higher potential difference imposed between the anodes and cathodes in microbial electrolysis cells can explain the microbial diversity observed in our case. Enrichment of *Geobacter* spp. occurred on the anodes, and this was expected as these species are very well known for harvesting electricity on anodes [34]. Some *Geobacter* spp. can utilize hydrogen as an electron donor and some can even produce hydrogen under certain conditions [35]. Hydrogen was produced on the MEC cathodes; however, since the main electron acceptors available close to the cathodes were protons and carbon dioxide, it is reasonable that no *Geobacter* spp. were detected on any of the cathodes. On the other hand, γ-Proteobacteria were very much enriched in the dual-chamber cathode, and these have also been found elsewhere to dominate anoxic microbial fuel cell cathodes [34]. *Acetobacterium* spp. and *Acetoanaerobium* spp., which can utilize $H_2$ and $CO_2$ for the production of acetate under anaerobic conditions [36,37], were found on the sliced membrane reactor cathode, but not on the membraneless reactor cathode. Hydrogen (approximately 10% of the biogas) was produced in both reactors and could potentially be used by these bacterial species on both MEC cathodes. However, though acetogenesis might have occurred at a limited degree, it did not seem to hinder COD removal and methane production in the membraneless MEC reactor. In other studies where anodes of dual-chamber MECs were fed with a fermentable substrate [38,39], it was shown that homo-acetogens were producing acetate from hydrogen and carbon dioxide, only when methanogenesis was inhibited. However, in our sliced membrane reactor acetogenesis and methanogenesis took place at the same time, and both were consuming electrons originating from the cathode.

While the cathode potentials applied on the membraneless reactor cathode promoted methane production, lower cathode potentials were shown to favor acetogenesis in the dual-chamber MEC cathode and in the H-type WE chamber. In the case of the membraneless MEC, the cathode potentials applied were maintained low enough for hydrogen and methane production but not low enough to stimulate acetogenesis at levels that would be problematic. In comparison, cathode potentials observed in similar methanogenic MECs were approximately between −820 and −900 mV [8]. When the homoacetogen *Acetobacterium woodii* was tested for acetate production in a cathode poised at the high cathode potential of −400 mV [40], it was found incapable of utilizing the electrode for acetate production. This was in contrast to other pure cultures that were tested (e.g. *Sporomusa* species), and even though the authors did not test lower electrode potentials, these findings are in agreement with our study.

In our H-type reactor, *Acetobacterium* spp. dominated the working electrode and these results are in agreement with the study of Marshall and colleagues [12], who found that *Acetobacterium* spp. were the dominant species on graphite granule electrodes (up to approximately 60%) when acetogenesis was dominant, but not in the suspension of a hydrogen, methane and acetate co-producing cathode. In addition, the presence of *Acetobacterium* spp. in the H-type WE chamber shows that these bacteria were present in the suspension of the membraneless MEC that was used as inoculum, however they could not thrive on the cathode of the membraneless MEC, which was maintained at potentials higher than −920 mV. On the contrary, they dominated the H-type WE and were driving electrons towards acetate production when the WE potential was equal or lower than −1000 mV. Furthermore, *Acetobacterium* spp. were not dominant in the suspension of the H-type cell cathode (approximately 2%; data not shown), most probably because hydrogen was constantly being removed from the system by vigorous $CO_2$ sparging.

Whether homoacetogens can directly accept electrons from a poised electrode for the production of acetate is yet to been shown at a molecular level; however, if they do, membrane-bound cytochromes and cobalt-containing corrinoids [41–43] might be involved, requiring appropriately low electrode potentials for their reduction–oxidation cycles. Direct utilization of the electrode could be possible, however other mechanisms like interspecies direct hydrogen transfer from hydrogen producing bacteria cannot be excluded at this point, and further investigation is needed. Still, acetogenesis was not an issue in the membraneless system which was also producing hydrogen, a potential electron donor for the acetogens.

Increasing acetogenesis with decreasing electrode potentials will potentially fail single-chamber MECs designed for COD removal and energy production. Since acetogenesis was dominant at lower potentials than methanogenesis did, then a way of controlling acetogenesis would be by maintaining the cathode potentials high enough but at levels that would allow sufficient hydrogen and methane production. A way to achieve this would be by increasing the cathode to anode surface area ratio in order to control the current density demanded by the anode. Decreasing the internal resistance of the system (e.g. by removing the membrane, improving the cathode materials, etc.) is also expected to have a positive effect, as it would decrease the electrical pressure applied on the cathode.

## Conclusions

MECs can produce net energy and enhance methanogenesis and COD removal, however acetogenesis can be problematic and should be controlled. Small differences in the applied conditions (e.g. electrode potentials, pH) can have a decisive effect on the bacterial enrichment, as they will create different micro-environments that will allow the development of diverse microbial communities. Acetogens grown under favorable cathode conditions can decrease the energy efficiency of MEC systems and increase the COD in the effluent of membraneless systems designed for wastewater treatment on the anode. For this reason, controlling the cathode potentials is equally important as controlling the anode potentials, and higher current production does not always come with higher COD reduction rates. More research is needed in order to better optimize and control the processes involved, particularly with regards to the electron transfer mechanisms of the

cathodophilic microbes; in other words, how they interact with the poised electrode, and what the microbial syntrophy on the cathode involves. Besides making wastewater treatment more energy efficient, understanding the mechanisms involved will also allow us to optimize other microbial electrosynthesis processes taking place in the cathode.

## Acknowledgments

Funding in support of this work was provided by Göteborg Energi Forskningsstiftelsen (Project N° 11-16), Gothenburg, Sweden. The authors would like to thank Professor Carlo Mapelli from the Politecnico di Milano for providing us with the graphite blocks, Dr Yue Zhang from the University of Southampton for lending us the single-channel potentiostat, and also Gryaab AB (Gothenburg, Sweden) for providing us with the anaerobic sludge. We would also like to express our gratitude to Agnieszka Krain for assisting with the microbial characterization of the anaerobic sludge.

## REFERENCES

[1] Li WW, Yu HQ, He Z. Towards sustainable wastewater treatment by using microbial fuel cells-centered technologies. Energy Environ Sci 2014;7:911–24.
[2] Xafenias N, Zhang Y, Banks CJ. Enhanced performance of hexavalent chromium reducing cathodes in the presence of *Shewanella oneidensis* MR-1 and lactate. Environ Sci Technol 2013;47:4512–20.
[3] Han Y, Yu C, Liu H. A microbial fuel cell as power supply for implantable medical devices. Biosens Bioelectron 2010;25:2156–60.
[4] Ieropoulos IA, Greenman J, Melhuish C, Horsfield I. Microbial fuel cells for robotics: energy autonomy through artificial symbiosis. ChemSusChem 2012;5:1020–6.
[5] Ieropoulos IA, Ledezma P, Stinchcombe A, Papaharalabos G, Melhuish C, Greenman J. Waste to real energy: the first MFC powered mobile phone. Phys Chem Chem Phys 2013;15:15312.
[6] Lovley DR, Nevin KP. Electrobiocommodities: powering microbial production of fuels and commodity chemicals from carbon dioxide with electricity. Curr Opin Biotechnol 2013;24:385–90.
[7] Logan BE, Call D, Cheng S, Hamelers HVM, Sleutels THJA, Jeremiasse AW, et al. Microbial electrolysis cells for high yield hydrogen gas production from organic matter. Environ Sci Technol 2008;42:8630–40.
[8] Clauwaert P, Verstraete W. Methanogenesis in membraneless microbial electrolysis cells. Appl Microbiol Biotechnol 2009;82:829–36.
[9] Eerten-Jansen MCAAV, Veldhoen AB, Plugge CM, Stams AJM, Buisman CJN, Heijne AT. Microbial community analysis of a methane-producing biocathode in a bioelectrochemical system. Archaea; 2013:1–12.
[10] Santoro C, Cremins M, Pasaogullari U, Guilizzoni M, Casalegno A, Mackay A, et al. Evaluation of water transport and oxygen presence in single chamber microbial fuel cells with carbon-based cathodes. J Electrochem Soc 2013;160:3128.
[11] Cristiani P, Carvalho ML, Guerrini E, Daghio M, Santoro C, Li B. Cathodic and anodic biofilms in single chamber microbial fuel cells. Bioelectrochemistry 2013;92:6–13.
[12] Marshall CW, Ross DE, Fichot EB, Norman RS, May HD. Electrosynthesis of commodity chemicals by an autotrophic microbial community. Appl Environ Microbiol 2012;78:8412–20.
[13] Tartakovsky B, Mehta P, Bourque JS, Guiot SR. Electrolysis-enhanced anaerobic digestion of wastewater. Bioresour Technol 2011;102:5685–91.
[14] Hu H, Fan Y, Liu H. Hydrogen production using single-chamber membrane-free microbial electrolysis cells. Water Res 2008;42:4172–8.
[15] Call D, Logan BE. Hydrogen production in a single chamber microbial electrolysis cell lacking a membrane. Environ Sci Technol 2008;42:3401–6.
[16] Lu L, Ren N, Zhao X, Wang H, Wu D, Xing D. Hydrogen production, methanogen inhibition and microbial community structures in psychrophilic single-chamber microbial electrolysis cells. Energy Environ Sci 2011;4:1329.
[17] Guo X, Liu J, Xiao B. Bioelectrochemical enhancement of hydrogen and methane production from the anaerobic digestion of sewage sludge in single-chamber membrane-free microbial electrolysis cells. Int J Hydrogen Energy 2013;38:1342–7.
[18] Liang DW, Peng SK, Lu SF, Liu YY, Lan F, Xiang Y. Enhancement of hydrogen production in a single chamber microbial electrolysis cell through anode arrangement optimization. Bioresour Technol 2011;102:10881–5.
[19] Lu L, Xing D, Ren N. Bioreactor performance and quantitative analysis of methanogenic and bacterial community dynamics in microbial electrolysis cells during large temperature fluctuations. Environ Sci Technol 2012;46:6874–81.
[20] Lee HS, Rittmann BE. Significance of biological hydrogen oxidation in a continuous single-chamber microbial electrolysis cell. Environ Sci Technol 2010;44:948–54.
[21] Rader GK, Logan BE. Multi-electrode continuous flow microbial electrolysis cell for biogas production from acetate. Int J Hydrogen Energy 2010;35:8848–54.
[22] Sasaki K, Morita M, Sasaki D, Matsumoto N, Ohmura N, Igarashi Y. Single-chamber bioelectrochemical hydrogen fermentation from garbage slurry. Biochem Eng J 2012;68:104–8.
[23] Sasaki K, Morita M, Sasaki D, Ohmura N, Igarashi Y. The membraneless bioelectrochemical reactor stimulates hydrogen fermentation by inhibiting methanogenic archaea. Appl Microbiol Biotechnol 2013;97:7005–13.
[24] Sasaki K, Morita M, Matsumoto N, Sasaki D, Hirano S, Ohmura N, et al. Construction of hydrogen fermentation from garbage slurry using the membrane free bioelectrochemical system. J Biosci Bioeng 2012;114:64–9.
[25] Lee HS, Torres CI, Parameswaran P, Rittmann BE. Fate of $H_2$ in an upflow single-chamber microbial electrolysis cell using a metal-catalyst-free cathode. Environ Sci Technol 2009;43:7971–6.
[26] APHA. Standard methods for the examination of water and wastewater. Washington DC: American Public Health Association (APHA), American Water Works Association (AWWA), Water Environment Federation (WEF); 2005.
[27] Weisburg WG, Barns SM, Pelletier DA, Lane DJ. 16S ribosomal DNA amplification for phylogenetic study. J Bacteriol 1991;173:697–703.
[28] Neilan BA, Jacobs D, Del Dot T, Blackall LL, Hawkins PR, Cox PT, et al. rRNA sequences and evolutionary relationships among toxic and nontoxic cyanobacteria of the genus *Microcystis*. Int J Syst Bacteriol 1997;47:693–7.

[29] Short JM, Fernandez JM, Sorge JA, Huse WD. λ ZAP: a bacteriophage λ expression vector within vivo excision properties. Nucleic Acids Res 1988;16:7583–600.
[30] Cole JR, Wang Q, Fish JA, Chai B, McGarrell DM, Sun Y, et al. Ribosomal database project: data and tools for high throughput rRNA analysis. Nucleic Acids Res 2013;42:633.
[31] Wang Q, Garrity GM, Tiedje JM, Cole JR. Naive Bayesian classifier for rapid assignment of rRNA sequences into the new bacterial taxonomy. Appl Environ Microbiol 2007;73:5261–7.
[32] Clauwaert P, Toledo R, van der Ha D, Crab R, Verstraete W, Hu H, et al. Combining biocatalyzed electrolysis with anaerobic digestion. Water Sci Technol 2008;57:575–9.
[33] Cristiani P, Franzetti A, Gandolfi I, Guerrini E, Bestetti G. Bacterial DGGE fingerprints of biofilms on electrodes of membraneless microbial fuel cells. Int Biodeterior Biodegradation 2013;84:211–9.
[34] Holmes DE, Bond DR, O'Neil RA, Reimers CE, Tender LR, Lovley DR. Microbial communities associated with electrodes harvesting electricity from a variety of aquatic sediments. Microb Ecol 2004;48:178–90.
[35] Coppi MV. The hydrogenases of Geobacter sulfurreducens: a comparative genomic perspective. Microbiol Sgm 2005;151:1239–54.
[36] Sleat R, Mah RA, Robinson R. *Acetoanaerobium noterae* gen. nov., sp. nov.: an anaerobic bacterium that forms acetate from $H_2$ and $CO_2$. Int J Syst Bacteriol 1985;35:10–5.
[37] Balch WE, Schoberth S, Tanner RS, Wolfe RS. Acetobacterium, a new genus of hydrogen-oxidizing, carbon dioxide-reducing, anaerobic bacteria. Int J Syst Bacteriol 1977;27:355–61.
[38] Parameswaran P, Torres CI, Lee HS, Krajmalnik-Brown R, Rittmann BE. Syntrophic interactions among anode respiring bacteria (ARB) and non-ARB in a biofilm anode: electron balances. Biotechnol Bioeng 2009;103:513–23.
[39] Parameswaran P, Zhang H, Torres CI, Rittmann BE, Krajmalnik-Brown R. Microbial community structure in a biofilm anode fed with a fermentable substrate: the significance of hydrogen scavengers. Biotechnol Bioeng 2010;105:69–78.
[40] Nevin KP, Hensley SA, Franks AE, Summers ZM, Ou J, Woodard TL, et al. Electrosynthesis of organic compounds from carbon dioxide is catalyzed by a diversity of acetogenic microorganisms. Appl Environ Microbiol 2011;77:2882–6.
[41] Drake HL. Acetogenesis. US: Springer; 1995.
[42] Ragsdale SW, Pierce E. Acetogenesis and the Wood–Ljungdahl pathway of $CO_2$ fixation. Biochim Biophys Acta 2008;1784:1873–98.
[43] Ragsdale SW. Enzymology of the Wood-Ljungdahl pathway of acetogenesis. Ann N Y Acad Sci 2008;1125:129–36.